Measured and Predicted Unsaturated Permeability of Cracked Compacted Fine Soil

Abdelkader Mabrouk
Civil Engineering Department, College of Engineering, Northern Border University, Saudi Arabia
abdjih2019@gmail.com (corresponding author)

Mehrez Jamei
Civil Engineering Department, College of Engineering, Northern Border University, Saudi Arabia
mehjamei@yahoo.fr

Anwar Ahmed
Civil Engineering Department, College of Engineering, Northern Border University, Saudi Arabia
anah66432@gmail.com

Received: 1 March 2024 | Revised: 18 March 2024 | Accepted: 27 March 2024

 DOI: https://doi.org/10.48084/etasr.7178

ABSTRACT

The unsaturated permeability of cracked compacted fine soil is a key parameter in geotechnical engineering, particularly when analyzing water flow through the soil in various conditions. The compaction affects the saturated and unsaturated permeability by reducing porosity. However, cracks can appear by shrinkage and growth during desiccation, which obviously leads to macro-porosity (a process during which the soil acquires a high level of double porosity). The development of a crack network influences the suction (as negative water pressure) and then the unsaturated permeability. The current paper aims to analyze the role of the crack network (considered as macropores) on the unsaturated permeability, by quantifying the network based on the Crack Intensity Factor (CIF). The unsaturated permeability is given as a function, separately of CIF and suction. The experimental results may be considered constructive for soil modeling. Regarding the birth of the first crack, it occurred when the suction reached a value near to that of the air entry suction. Since the first crack appeared, primary cracks were developed and then followed by secondary cracks. The obtained experimental results of WRC and K_{unsat} for cracked compacted clay are beneficial in managing the design of the geotechnical structure stability and the environmental issues of water diffusion. CIF increases with suction, which is augmented during the drying process demonstrating a decrease in the moisture content. After 21 hours of desiccation, CIF ended up reaching a value of 4%. It is generally recognized that cracks create preferential pathways for water flow, whereas their geometry and distribution influence how water moves through the soil. Modeling the impact of cracks on permeability may involve considering factors like crack width, orientation, and connectivity. In this paper, a simple model was proposed to predict the unsaturated permeability as a function of suction with different CIF values with the material being assumed as a double porosity soil.

Keywords-unsaturated permeability; desiccation; cracks; water retention; compaction; double porosity

I. INTRODUCTION

The sustainability issue of several geotechnical works is linked to soil permeability, which is entirely dependent on the soil structure type, the former's mineralogy and fabric [1-3] and also on the interactions, at microstructure and macrostructure scales, between the water and the soil particles (the swelling and the shrinkage of clays are mentioned as a non-exhaustive example, where the interaction between particles and water plays a crucial role on the deformation rate). For instance, regarding the active clay, the opposite phenomena observed, such as swelling and shrinkage, may be the origin of macro-porosity creation. In the case of swelling, macro-porosity is induced by the double-layer action. The provided by shrinkage cracks are also assumed as macropores with the same equivalent volume [4-6]. Considering shrinkage, the tensile deformations leading to cracks result from heterogeneity of moisture water content, density, and eventually from the external mechanical boundary conditions [7]. The cracks' development and growth significantly affect the hydraulic properties, namely saturated permeability, unsaturated permeability, and water retention [8-12]. Laboratory testing involving instruments like a constant head or a falling head permeameter is commonly used to measure water flow through

the soil samples [13]. However, in the case of unsaturated cracked soil, the flow mainly happens in a transient state. So, more attention should be placed on the suction's evolution during the flow test about the cracks. Such an experimental procedure could be complex since the soil porosity changes with the crack network evolution during a drying path or a drying-wetting cycle. It is not common to simultaneously follow both the crack growth and the evaporation flux to determine the unsaturated permeability. One powerful technique to achieve this is to use the evaporation method by applying a gradient suction on the cracked specimen [14-16]. The translate method, which involves utilizing a gradient suction on a cracked specimen, has been also applied [17]. Regarding the role of initial unsaturated conditions of the prepared soil specimens, it was demonstrated that the initial water content and the initial dry density govern the crack network and the Crack Intensity Factor (CIF), which is defined as the rate between the volume of cracks and the total volume of the specimen. Consequently, the presence of cracks in compacted fine soil can significantly affect its permeability [18, 19]. On the other hand, predicting unsaturated permeability often involves employing mathematical models, such as those based on soil characteristic curves, which describe the relationship among soil moisture content, suction, and permeability. Phenomenological models like the van Genuchten-Mualem or the Brooks-Corey model are commonly implemented for this purpose [20].

Despite the complexity of measuring the water content property and the unsaturated permeability for fine soils without cracking, several new procedures have been proposed [21, 22]. However, few studies have investigated the unsaturated permeability and water retention. Thus, the current research aims to experimentally contribute in the study of cracked compacted clay in order to characterize the main hydraulic properties of cracked soil. The expected results can be exploited in the design and modeling of environmental cases of geotechnical structures submitted to desiccation.

New experimental laboratory results are presented, to assist in studying the role of the crack network on the unsaturated silty soil permeability. Starting from initial homogenous soil conditions (compacted dry density and initial moisture water content), the saturated and unsaturated permeability function and the Soil-Water Retention Characteristic (SWRC) were experimentally determined for the intact specimens (without cracking). The specimens were then submitted to a water drying path, and the shrinkage was developed by conducting crack networks. The evaporation technique mentioned above determines the unsaturated permeability at a given crack network. These tests were performed for various crack network intensities (quantified by the CIF). The mixing law was applied engaging the Genuchten-Mualem model to predict the unsaturated permeability of more macroscopic levels, involving specimens with more important dimensions than those studied in the laboratory. The results were interpreted in terms of the CIF influence and suction variation.

II. EXPERIMENTAL STUDY

A. Materials and Experimental Protocol

The main physical soil properties are summarized in Table I. The Grain Size Distribution (GSD) curve is given in Figure 1. Based on the GSD and the properties of Table I, the soil is classified as silt with high plasticity and contains a significant percentage of organic matter (ASTM D 2487-17). The high plastic silt property is similar to the high activity of the silt, which generates the expectation of a high shrinkage potential. The Proctor compaction curve demonstrates the optimum compaction parameters, where $\gamma_{d,max}$ = 1.52 gr/cm^3. Additionally, the Optimum Moisture Content (OMC) is OMC = 25% (Figure 2). In the field's works, it is generally required to compact the soil in the range of 0.85×$\gamma_{d,max}$ to $\gamma_{d,max}$. Thus, the compaction dry unit weight value was fixed at 0.9×$\gamma_{d,max}$. Consequently, the moisture water content could approximately range from 16% to 32% (Figure 2). The zero-air voids curve (for a degree of saturation s_r = 1) is also plotted in Figure 2. The tested clay contains a high amount of smectite (around 60%) which explains its high activity and its high shrinkage potential.

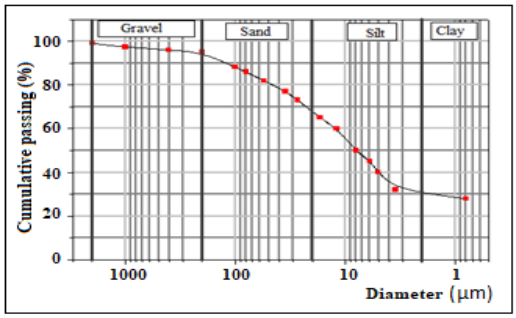

Fig. 1. Grain size distribution.

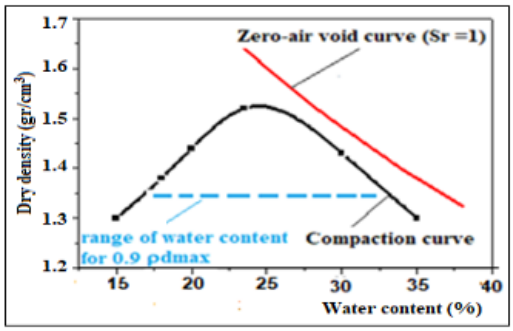

Fig. 2. Proctor compaction curve.

TABLE I. MAIN PHYSICAL AND CHEMICAL CHARACTERISTICS OF THE STUDIED SOIL

Shrinkage Limit (SL) (%)	Plastic Limit (PL) (%)	Liquid Limit (LL) (%)	Specific gravity (Gs)	$CaCo_3$ (%)	VBS	Activity (%)
15	35	72	2.68	16	7	77

Added to the previous main characteristics of the silt, the main unsaturated soil properties were measured in the laboratory to determine the water retention curve and the

unsaturated permeability function. The water retention curves for the matrix (soil without cracks) and cracked specimens were obtained using complementary measurement techniques, such as osmotic and filter paper methods [21-23]. The unsaturated permeability functions were identified according to the evaporation experience method [24]. The influence of the compacted clay was also investigated [24, 25].

B. Experimental Results

1) Intact Compacted Soil (Soil without Cracking)

The water retention curves for matrix and cracked soil were acquired and expressed as a relationship between the mass water content and suction. (for details of the experimental procedure see [26]). Figure 3 provides the water retention of the matrix. Two parameters are necessary to retain from the experimental results: the Air Entry Suction (AES) value and the residual suction (s_r). These values are around 300 KPa and 10 MPa, respectively. Using the van Genuchten (1980) [20] model permits the transition from the water retention equation to predict the unsaturated permeability. The van-Genuchten equation is obtained by utilizing the experimental results of the unsaturated permeability function against suction.

$$\theta^* = \frac{\theta-\theta_r}{\theta_s-\theta_r} = \left(\frac{1}{[1+(\alpha^* s)^n]^m}\right) = w^* \quad (1)$$

where $\theta = Gs \times w$ is the volumetric water content, where Gs is the specific gravity and w is the mass water content. θ_s and θ_r are the volumetric water content at saturation and the residual volumetric water content, correspondingly. From the SWRC of the matrix, w_s and $w_r$are 40% and 5%, accordingly. The van-Genuchten model was fitted, and its coefficients are n = 1.65 and α^* =0.005 cm^{-1} (m = 1-1/n). The unsaturated permeability was fitted according to (2), and is plotted in Figure 4.

$$k_{ns}(s) = k_s \frac{1-(\alpha s)^{n-2}[1+(\alpha s)^n]^{-m}}{[1+(\alpha s)^n]^{2m}} \quad (2)$$

where k_s is the saturated permeability measured by the falling permeameter (k_s = 1.5 10^{-10} m/s).

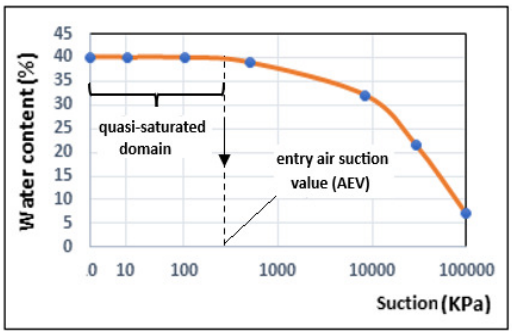

Fig. 3. Water retention of the intact soil.

Microscopic observation is presented at the end of the compaction stage. Figure 5 gives the SEM view of the sample after its compaction at the density of $\gamma_{d,max}$ = 1.52 gr/cm^3. The results clearly exhibit two aspects: the texture of the soil and the double porosity character of the compacted silt and clay. Some previous studies have demonstrated the double porosity property of the compacted fine soil's micros-texture [23]. Microporosity characterizes the voids between the particles. However, macroporosity corresponds to the voids between agglomerates (set of embedded participles).

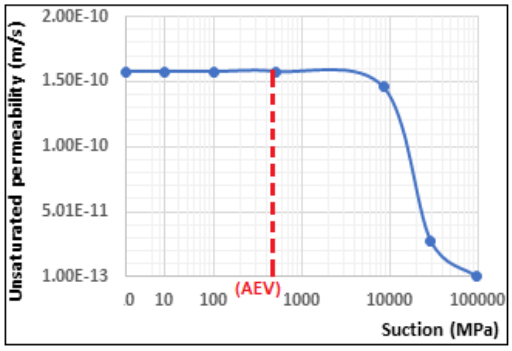

Fig. 4. Unsaturated permeability of the intact soil.

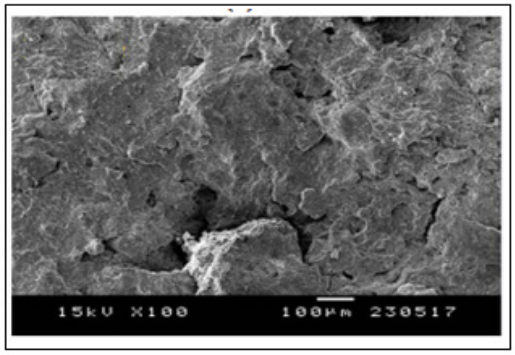

Fig. 5. SEM view of the microstructure of a compacted specimen at $\gamma_{d,max}$=1.52 gr/cm^3.

2) Cracked Compacted Soil

Regarding the experimental study of the cracks' effect on the saturated and unsaturated permeability of the compacted soil, several tests were conducted to measure the impact of the network cracks. The experimental procedure was defined as follows: (a) the samples were compacted at the desired dry density, (b) the specimens prepared at the given density were placed in an environmental chamber, where the temperature was fixed, and the Relative Humidity (RH) was controlled, (c) a series of photos was taken during the desiccation time by a camera placed in the environmental chamber, (d) image analysis was applied to define network characteristics, such as the opening, the length, and the diffusion angles and orientations of the cracks (for more details about the image analysis see [27]). Consequently, the CIF was deduced during this time, as observed in Figures 6 and 7. Figure 6 depicts the procedure for compacting the specimen and the following stages for applying the drainage path. Image analysis was performed at each reached cracking level. Temperature T was fixed at 30 °C ± 5 °C and the relative humidity was 50% ± 5%.

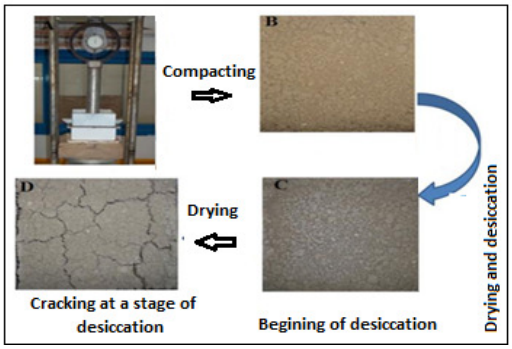

Fig. 6. Procedure followed to detect the crack network.

Figure 7 presents the crack network for a dry density γ_d =1.35 gr/cm^3 as well as primary and secondary fissures form the crack network. The angles between the cracks are between 60° and 120°. The compaction enhanced the macropores in the non-fissured zone.

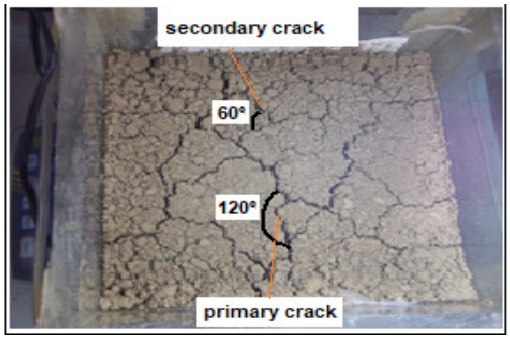

Fig. 7. Crack network at the end of desiccation (compacted specimen γ_d = 1.35 gr/cm^3).

The 3D CIF is:

$$CIF = \frac{\text{Cracks volume}}{\text{Total volume}} \quad (3a)$$

The 2D CIF is:

$$CIF = \frac{\text{Cracks area}}{\text{Total area}} \quad (3b)$$

Figure 8 portrays the evolution of CIF (determined in 2D) against the suction during desiccation. As observed, the CIF increases with suction, which is augmented during the drying process with a decrease in the moisture content. At the end of the desiccation, that is, after 21 hours, CIF reached a value of 4%. As it can be deduced, the maximum CIF for compacted soil is commonly less than the maximum CIF that can be reached for the slurry soil. However, the spatial variability of cracks is generally more homogeneous. The former covers all the compacted layers or specimens, opposite the slurry soil case where the crack network is more concentrated in the local space, depending on the boundary conditions or the local density and the water content heterogeneity. The measurement of the permeability of the compacted cracked specimens (Figure 6) was also performed at CIF= 4%, with results regarding unsaturated permeability against suction (Figure 9). As expected, the permeability significantly increased compared to the intact matrix's unsaturated permeability (Figure 4).

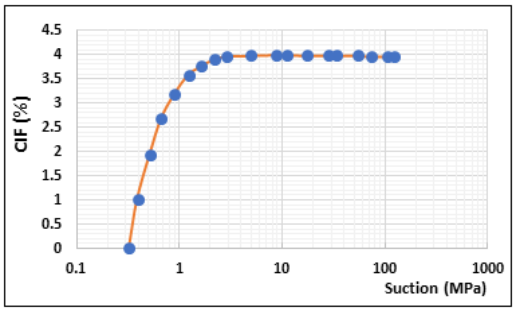

Fig. 8. CIF against suction.

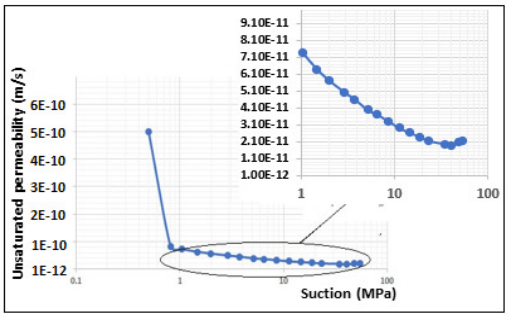

Fig. 9. Unsaturated permeability of the cracked specimen (CIF=4%).

Figure 10 also confirms the aforementioned expectation, showing that unsaturated permeability decreases with increasing CIF. Cracks create preferential pathways for water flow, and their geometry and distribution influence the way water moves through the soil. Modeling the impact of cracks on permeability may involve considering factors like crack width, orientation, and connectivity.

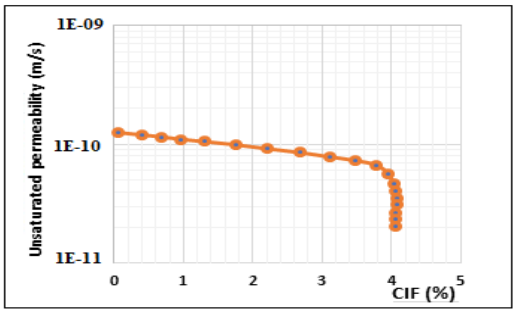

Fig. 10. Unsaturated permeability of the cracked specimen against CIF.

III. MODELING

Modeling is usually expected to be practiced for complex physical problems such as predicting the unsaturated permeability of large scale dimensions of the geotechnical structure and large scale volume of the soil (as a non-exhaustive example, in [28], some empirical equations were proposed to predict the unsaturated soil permeability from the water retention curve). A simple mixing model introduces permeability functions, namely the unsaturated permeability of cracked specimens at a small scale and the unsaturated

permeability of intact soil matrix. The model is written as follows:

$$\tilde{K}_{n,S}(s) = (1-CIF).K_{matrix} + CIF.K_{cracks} \quad (4)$$

$$K_{matrix} = K_{s,matrix} k_{ns,matrix} = \\ = K_{s,matrix} \frac{1-(\alpha_1 s)^{n-2}[1+(\alpha_1 s)^n]^{-m}}{[1+(\alpha_1 s)^n]^{2m}} \quad (5)$$

where n = 1.65, m = 0.39, a_1 = 0.005 cm^{-1}, and $K_{s,matrix}$ = 1.5×10^{-10} m/s.

$$K_{cracks} = K_{s,cracks} k_{ns,cracks} = \\ = K_{s,cracks} \frac{1-(\alpha_2 s)^{n-2}[1+(\alpha_2 s)^n]^{-m}}{[1+(\alpha_2 s)^n]^{2m}} \quad (6)$$

where n = 2.08, m = 0.52, a_2 = 0.01 cm^{-1}, and $K_{s,matrix}$ = 2×10^{-6} m/s.

Equation (4) is available only for the suction over a threshold value, defined as the suction where the first crack appears. To simplify this process, it is admitted that in the model the threshold value equals the air-entry suction (AEV). The results are summarized in Figure 11, which indicates that the predicted unsaturated equivalent permeability $\widetilde{k\_ns}(s)$ remains not far from the intact matrix permeability. The equivalent unsaturated permeability function $\widetilde{k\_ns}(s)$ is significantly depended on CIF. This demonstrates anew the importance of the prediction at the large scale of the equivalent permeability and quantifys it for reliable geotechnical structures.

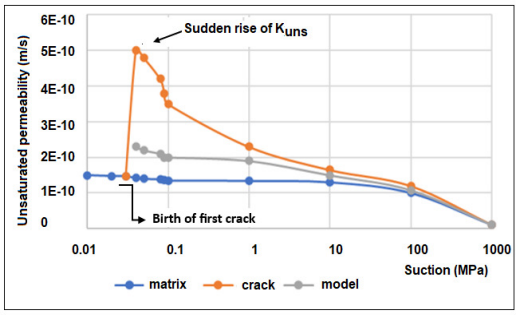

Fig. 11. Predicted equivalent unsaturated permeability function (against suction).

Since the first crack appears (birth), the permeability value suddenly jumps and increases (from 1.3×10^{-10} m/s to 5×10^{-10} m/s). The unsaturated permeability of the cracked specimen decreases with suction until reaching the K_{unsat} of the matrix. This means that at a high suction value (about 100 MPa) the developed cracks do not contribute to the water flow and become resistant.

IV. CONCLUSION

The results obtained across this study concerned the experimental determination of:

1. The Soil-Water Retention Curve (SWRC) and the unsaturated permeability. The key parameters of the air-suction value (AEV) functions, residual suction, saturated water content, and saturated permeability, were obtained. The van Genuchten-Mualem model was used to fit the experimental curves, where the parameters were calibrated.
2. The birth of the first crack occurred when the suction reached a value nearly the AEV. Since the first crack appeared, a primary crack network was developed followed by secondary cracks. The acquired experimental results of WRC and K_{unsat} for compacted clay are valuable for the management of the design of geotechnical structure stability and the environmental issues of water diffusion (e.g. a landfill cover).
3. The effect of the Crack Intensity Factor (CIF) obtained for the compacted specimens on the unsaturated permeability was well demonstrated. The unsaturated permeability increases with CIF.
4. CIF increases with suction, which raises during the drying process with a decrease in the moisture content. After 21 hours of desiccation, CIF reached a value of 4%.
5. Cracks create preferential pathways for water flow, and their geometry and distribution influence how water moves through the soil. Modeling the impact of cracks on permeability may involve considering factors like crack width, orientation, and connectivity.
6. The mixing law was a simple approximation of the prediction of the unsaturated permeability of the soil with large-scale dimensions compared to the cracked specimen's dimensions. This law predicted the effective unsaturated permeability dependency on CIF.
7. Due to the random distribution of cracks, the convenient randomly homogeneous theory will be envisaged to predict K_{unsat} and WRC.

ACKNOWLEDGMENT

The authors gratefully acknowledge the approval and the support of this research study by the grant no. ENGA-2022-11-1762 from the Deanship of Scientific Research at Northern Border University, Arar, K.S.A.

REFERENCES

[1] N. Kumari and C. Mohan, "Basics of clay minerals and their characteristic properties," in *Clay and Clay Minerals*, G. M. D. Nascimento, Ed. London, UK: IntechOpen, 2021, pp. 15–44.

[2] K. A. Morris and C. M. Shepperd, "The role of clay minerals in influencing porosity and permeability characteristics in the Bridport Sands of Wytch Farm, Dorset," *Clay Minerals*, vol. 17, no. 1, pp. 41–54, Mar. 1982, https://doi.org/10.1180/claymin.1982.017.1.05.

[3] N. A. Tuan and P. Q. Chieu, "The Effect of Moisture and Fine Grain Content on the Resilient Modulus of Sandy Clay Embankment Roadbed," *Engineering, Technology & Applied Science Research*, vol. 11, no. 3, pp. 7118–7124, Jun. 2021, https://doi.org/10.48084/etasr.4152.

[4] A. Sridharan and M. S. Jayadeva, "Double layer theory and compressibility of clays," *Géotechnique*, vol. 32, no. 2, pp. 133–144, Jun. 1982, https://doi.org/10.1680/geot.1982.32.2.133.

[5] R. Lopez-Vizcaino *et al.*, "A modeling approach for electrokinetic transport in double-porosity media," *Electrochimica Acta*, vol. 431, Nov. 2022, Art. no. 141139, https://doi.org/10.1016/j.electacta.2022.141139.

[6] Y. Wan, J. Kwong, H. G. Brandes, and R. C. Jones, "Influence of Amorphous Clay-Size Materials on Soil Plasticity and Shrink-Swell Behavior," *Journal of Geotechnical and Geoenvironmental Engineering*, vol. 128, no. 12, pp. 1026–1031, Dec. 2002, https://doi.org/10.1061/(ASCE)1090-0241(2002)128:12(1026).

[7] H. Trabelsi, M. Jamei, H. Zenzri, and S. Olivella, "Crack patterns in clayey soils: Experiments and modeling," *International Journal for Numerical and Analytical Methods in Geomechanics*, vol. 36, no. 11, pp. 1410–1433, 2012, https://doi.org/10.1002/nag.1060.

[8] F. Louati, H. Trabelsi, M. Jamei, and S. Taibi, "Impact of wetting-drying cycles and cracks on the permeability of compacted clayey soil," *European Journal of Environmental and Civil Engineering*, vol. 25, no. 4, pp. 696–721, Mar. 2021, https://doi.org/10.1080/19648189.2018.1541144.

[9] N. Mangi, D. A. Mangnejo, H. Karira, M. Kumar, A. A. Jhatial, and F. R. Lakhair, "Crack Pattern Investigation in the Structural Members of a Framed Two-Floor Building due to Excavation-Induced Ground Movement," *Engineering, Technology & Applied Science Research*, vol. 9, no. 4, pp. 4463–4468, Aug. 2019, https://doi.org/10.48084/etasr.2923.

[10] N. P. Mahmoud and A. Zabihi, "Numerical Simulation of a Single-Phase Flow Through Fractures with Permeable, Porous and Non-Ductile Walls," *Engineering, Technology & Applied Science Research*, vol. 7, no. 5, pp. 2041–2046, Oct. 2017, https://doi.org/10.48084/etasr.1448.

[11] Y. Wang, D. Feng, and C. W. W. Ng, "Modeling the 3D crack network and anisotropic permeability of saturated cracked soil," *Computers and Geotechnics*, vol. 52, pp. 63–70, Jul. 2013, https://doi.org/10.1016/j.compgeo.2013.03.005.

[12] M. H. Rayhani, E. K. Yanful, and A. Fakher, "Desiccation-induced cracking and its effect on the hydraulic conductivity of clayey soils from Iran," *Canadian Geotechnical Journal*, vol. 44, no. 3, pp. 276–283, Mar. 2007, https://doi.org/10.1139/t06-125.

[13] F. Louati, A. Mabrouk, H. Trabelsi, M. Jamei, and H. Zenzri, "Flow exchange and unsaturated permeability of cracked clay: experimental and modelling," *European Journal of Environmental and Civil Engineering*, vol. 26, no. 15, pp. 7383–7399, Nov. 2022, https://doi.org/10.1080/19648189.2021.1989051.

[14] P. Pandey *et al.*, "Measurements of permeability of saturated and unsaturated soils," *Geotechnique*, vol. 71, no. 2, pp. 170–177, Feb. 2021, https://doi.org/10.1680/jgeot.19.P.058.

[15] F. Louati, H. Trabelsi, M. Jamei, and S. Taibi, "Impact of wetting-drying cycles and cracks on the permeability of compacted clayey soil," *European Journal of Environmental and Civil Engineering*, vol. 25, no. 4, pp. 696–721, Mar. 2021, https://doi.org/10.1080/19648189.2018.1541144.

[16] F. Louati, H. Trabelsi, M. Jamei, and A. N. Mabrouk, "Unsaturated permeability prediction using natural evaporation method in cracked clay," in *7th International Conference on Unsaturated Soils*, Hong Kong, China, Aug. 2018, pp. 1–7.

[17] F. Louati, "Etude experimentale et modelisation des proprietes hydriques d'une argile fissuree par dessiccation: Effet des cycles de drainage-humidification," Ph.D. dissertation, National Engineering School of Tunis, Tunis, Tunisia, 2019.

[18] X. Xing, W. Nie, K. Chang, L. Zhao, Y. Li, and X. Ma, "A numerical approach for modeling crack closure and infiltrated flow in cracked soils," *Soil and Tillage Research*, vol. 233, Sep. 2023, Art. no. 105794, https://doi.org/10.1016/j.still.2023.105794.

[19] J. H. Li, L. M. Zhang, and X. Li, "Soil-water characteristic curve and permeability function for unsaturated cracked soil," *Canadian Geotechnical Journal*, vol. 48, no. 7, pp. 1010–1031, Jul. 2011, https://doi.org/10.1139/t11-027.

[20] M. Th. van Genuchten, "A Closed-form Equation for Predicting the Hydraulic Conductivity of Unsaturated Soils," *Soil Science Society of America Journal*, vol. 44, no. 5, pp. 892–898, 1980, https://doi.org/10.2136/sssaj1980.03615995004400050002x.

[21] T. Wen, L. Shao, X. Guo, and Y. Zhao, "Experimental investigations of the soil water retention curve under multiple drying–wetting cycles," *Acta Geotechnica*, vol. 15, no. 11, pp. 3321–3326, Nov. 2020, https://doi.org/10.1007/s11440-020-00964-2.

[22] P. Delage and Y. J. Cui, "An evaluation of the osmotic method of controlling suction∗," *Geomechanics and Geoengineering*, vol. 3, no. 1, pp. 1–11, Feb. 2008, https://doi.org/10.1080/17486020701868379.

[23] E.-C. Leong, R. Kizza, and H. Rahardjo, "Measurement of soil suction using moist filter paper," *E3S Web of Conferences*, vol. 9, 2016, Art. no. 10012, https://doi.org/10.1051/e3sconf/20160910012.

[24] C. H. Benson and G. P. Boutwell, "Compaction Conditions and Scale-Dependent Hydraulic Conductivity of Compacted Clay Liners," in *Constructing and Controlling Compaction of Earth Fills*, West Conshohocken, PA, USA: ASTM International, 2000.

[25] Y. J. Cui, A. M. Tang, C. Loiseau, and P. Delage, "Determining the unsaturated hydraulic conductivity of a compacted sand–bentonite mixture under constant-volume and free-swell conditions," *Physics and Chemistry of the Earth, Parts A/B/C*, vol. 33, pp. S462–S471, Jan. 2008, https://doi.org/10.1016/j.pce.2008.10.017.

[26] M. M. Abbaszadeh, S. Houston, C. Zapata, W. Houston, B. Welfert, and K. Walsh, "Laboratory determination of Soil-Water Characteristic Curves for cracked soil: 5th International Conference on Unsaturated Soils," in *5th International Conference on Unsaturated Soils*, Barcelona, Spain, Sep. 2010, pp. 409–415.

[27] D. Al-Jeznawi, M. Sanchez, and A. J. Al-Taie, "Using Image Analysis Technique to Study the Effect of Boundary and Environment Conditions on Soil Cracking Mechanism," *Geotechnical and Geological Engineering*, vol. 39, no. 1, pp. 25–36, Jan. 2021, https://doi.org/10.1007/s10706-020-01376-5.

[28] D. G. Fredlund, A. Xing, and S. Huang, "Predicting the permeability function for unsaturated soils using the soil-water characteristic curve," *Canadian Geotechnical Journal*, vol. 31, no. 4, pp. 533–546, Aug. 1994, https://doi.org/10.1139/t94-062.